Journal of Libyan Academy Bani Walid 2025
مجلة الأكاديمية الليبية بني وليد
e-ISSN: 3104-3860
المجلد الأول، العدد الثاني، 2025

Frequency-Domain Signal Characterization for Fault Detection in Rotating Mechanical Systems Using Fourier-Based Decomposition Techniques

Adel Khalleefah Hamad Darmeesh *
Faculty Member, Department of Materials and Metallurgy Engineering, Ajdabiya University, Libya
*Corresponding author: adelsh123431@gamail.com, adelsh_dermesh@uoa.edu.ly

توصيف إشارة المجال الترددي للكشف عن الأعطال في الأنظمة الميكانيكية الدوارة باستخدام تقنيات التحليل القائمة على فوريير

عادل خليفة حمد درميش *
عضو هيئة التدريس، قسم هندسة المواد والمعادن، جامعة أجدابيا، ليبيا

Received: 24-02-2025; Accepted: 19-04-2025; Published: 08-05-2025

Abstract
This study presents a comprehensive approach to fault detection in rotating mechanical systems through frequency-domain signal analysis using Fourier-based decomposition techniques. Time-domain vibration signals acquired from rotating machinery are transformed into the frequency domain to extract characteristic spectral components indicative of system health. The methodology leverages Fast Fourier Transform (FFT) algorithms and harmonic decomposition to isolate anomalies associated with mechanical imbalances, misalignments, and bearing wear. Experimental data collected from controlled test rigs under varying operational conditions validate the effectiveness of the proposed signal processing framework. Results demonstrate that frequency-domain analysis significantly enhances fault detectability compared to traditional time-domain inspection methods. This work contributes to the advancement of condition monitoring strategies by providing a robust, interpretable, and computationally efficient diagnostic tool applicable in industrial settings.

Keywords: Fault Detection, Rotating Mechanical Systems, Fourier-Based, Decomposition Techniques.

الملخص
تقدم هذه الدراسة نهجا شاملا للكشف عن الأخطاء في الأنظمة الميكانيكية الدوارة من خلال تحليل إشارة مجال التردد باستخدام تقنيات التحلل المستندة إلى فوريه. يتم تحويل إشارات اهتزاز المجال الزمني المكتسبة من الآلات الدوارة إلى مجال التردد لاستخراج المكونات الطيفية المميزة التي تدل على صحة النظام. تعتمد المنهجية على خوارزميات تحويل فوريه السريع (FFT) والتحليل التوافقي لعزل الشذوذات المرتبطة باختلال التوازن الميكانيكي، واختلالات المحاذاة، وتآكل المحامل. وتُثبت البيانات التجريبية المُجمعة من منصات اختبار مُتحكم بها في ظل ظروف تشغيلية مُتنوعة فعالية إطار معالجة الإشارة المُقترح. وتُظهر النتائج أن تحليل النطاق الترددي يُعزز بشكل كبير من إمكانية اكتشاف الأعطال مُقارنةً بأساليب الفحص التقليدية في النطاق الزمني. ويُساهم هذا العمل في تطوير استراتيجيات مراقبة الحالة من خلال توفير أداة تشخيصية قوية وقابلة للتفسير وذات كفاءة حسابية عالية، قابلة للتطبيق في البيئات الصناعية.

الكلمات المفتاحية: اكتشاف الأعطال، الأنظمة الميكانيكية الدوارة، القائمة على فوريه، تقنيات التحليل.

1. Introduction

Rotating machinery forms the backbone of various industrial operations, including power generation, aerospace, and manufacturing [1], [2], [3], [4]. However, mechanical faults such as rotor imbalance, shaft misalignment, gear tooth wear, and bearing defects can lead to catastrophic failures if undetected [5], [6], [7], [8], [9], [10]. Early diagnosis through effective signal analysis is crucial for predictive maintenance and system reliability [11], [12], [13], [14], [15].

1.2 Problem Statement

Traditional time-domain signal analysis often lacks sensitivity to subtle changes in machine behavior [16], [17], [18], [19], [20]. Furthermore, complex interactions between mechanical components can obscure fault signatures, making interpretation difficult without advanced signal processing tools.

1.3 Research Objectives

- To develop a reliable signal processing framework for detecting mechanical faults.
- To apply Fourier-based decomposition techniques for transforming time-domain vibration data into meaningful frequency-domain representations.
- To validate the method experimentally using real-world mechanical system data.

1.4 Contribution

This research contributes an enhanced methodology for fault detection in rotating systems using frequency-domain characterization, offering both interpretability and computational efficiency [21], [22], [23], [24], [25]. The key contribution of this work lies in demonstrating how Fourier-based decomposition techniques can enhance fault detection accuracy and interpretability in rotating systems. By leveraging the FFT algorithm, the method transforms raw vibration data into a physically meaningful frequency spectrum, enabling early and precise identification of common mechanical faults. The approach offers computational efficiency, ease of implementation, and direct correlation between spectral features and mechanical behavior making it suitable for real-time industrial monitoring and predictive maintenance applications.

2. Literature Review

2.1 Signal Processing in Mechanical Diagnostics

A review of existing signal processing methodologies used in mechanical diagnostics, including time-domain statistics, wavelet transforms, Hilbert-Huang transforms, and envelope analysis [26], [27].

2.2 Fourier Analysis in Mechanical Systems

Discussion of classical Fourier series and its modern implementation via Fast Fourier Transform (FFT). Emphasis is placed on its role in identifying periodic components and harmonics in mechanical vibration signals [28], [29], [30].

2.3 Comparative Studies

Comparison of FFT-based approaches with other signal decomposition techniques in terms of accuracy, speed, and applicability to different types of mechanical faults.

3. Methodology

3.1 System Description

Description of the experimental setup: a laboratory-scale rotating machinery test rig equipped with accelerometers, tachometers, and data acquisition systems.

3.2 Data Acquisition

Table 1. Data Acquisition Overview.

Parameter	Details
Sampling Rate	10,000 Hz
Signal Duration	10 seconds
Total Samples	100,000
Sensors Used	Piezoelectric accelerometers (2 units)
Sensor Placement	Radial on left and right bearing housings
Tachometer	Optical/magnetic for RPM measurement
Operating Speed	1800 RPM (30 Hz)
Load	Constant (no variation)
Test Conditions	Healthy, Imbalance, Misalignment, Bearing Defect

3.3 Signal Preprocessing

Signal preprocessing is a crucial step in preparing raw vibration data for frequency-domain analysis using Fast Fourier Transform (FFT). This section outlines the key preprocessing techniques applied to enhance signal quality and reduce artifacts that could distort spectral interpretation.

Before applying FFT, raw vibration signals are often corrupted by high-frequency noise or electromagnetic interference. To mitigate this:

- **Analog Anti-Aliasing Filter**

Applied during data acquisition to remove frequencies above half the sampling rate (Nyquist frequency), preventing aliasing.

- **Digital Bandpass Filtering**

A digital filter may be applied post-acquisition to retain only the frequency range of interest (e.g., 0–500 Hz), removing low-frequency drift and high-frequency noise unrelated to fault signatures. Improve signal-to-noise ratio (SNR) and ensure accurate spectral representation.

- **Detrending**

Vibration signals may contain a DC offset or linear trend due to sensor bias or environmental factors.

Linear Detrending

The mean or linear component is removed from the signal:

$$x_{\text{detrended}}[n] = x[n] - \text{mean}(x)$$

- **Polynomial Detrending**

Higher-order polynomial fits can be subtracted to eliminate non-linear baseline drifts.

"Purpose: Eliminate low-frequency components not related to mechanical vibrations and prevent spectral leakage."

- **Windowing Functions**

When performing FFT, abrupt signal truncation at the beginning and end of the time record can cause spectral leakage, where energy from a single frequency spread into adjacent bins.

To reduce this effect, windowing functions are applied as below

- **Hanning Window**

$$w[n] = 0.5\left(1 - \cos\left(\frac{2\pi n}{N-1}\right)\right), n = 0,1,\dots,N-1$$

- Hamming Window

$$w[n] = 0.54 - 0.46\cos\left(\frac{2\pi n}{N-1}\right)$$

This research has applied both windows taper the signal at the edges to zero, reducing discontinuities.

3.4 Frequency Domain Transformation

Fundamentals of Fast Fourier Transform (FFT)

3.5 Fault Signature Extraction

Harmonic content analysis

Sideband detection

Amplitude modulation tracking

Comparison of healthy and faulty spectra

3.6 Classification Strategy

Use of threshold-based or machine learning-assisted classification of fault types using extracted spectral features.

4. Experimental Results and Discussion

Table 2. Measurement Points and Instrumentation.

Component	Details
Accelerometers	Piezoelectric type, mounted radially on bearing housings (X and Y axes)
Number of Sensors	2 (one per bearing housing)
Measurement Points	- Left bearing housing (radial) - Right bearing housing (radial)
Tachometer	Optical or magnetic type, used to measure shaft rotational speed (RPM)
Signal Direction	Radial acceleration (g) measured in horizontal plane
Sampling Rate	10,000 Hz
Signal Duration	10 seconds per trial (100,000 samples per signal)
Data Acquisition System	Multi-channel DAQ with synchronized sampling
Signal Conditioning	Analog filtering (anti-aliasing), amplification
Software Tools	Python for FFT, plotting, and fault analysis

4.1 Test Setup and Conditions

The experimental investigation was conducted on a laboratory-scale rotating machinery test rig equipped with a variable-speed motor driving a horizontal shaft supported by two rolling-element bearings. Accelerometers were mounted radially on both bearing housings to capture vibration data in the X and Y directions. Three fault conditions were simulated:

- Case 1: Healthy baseline condition
- Case 2: Mass-induced rotor imbalance
- Case 3: Angular misalignment between the motor and driven shaft
- Case 4: Inner race defect in one of the bearings

Data was acquired at a sampling rate of 10 kHz under steady-state operation at 1800 RPM. Each trial lasted 10 seconds, resulting in 100,000 data points per signal.

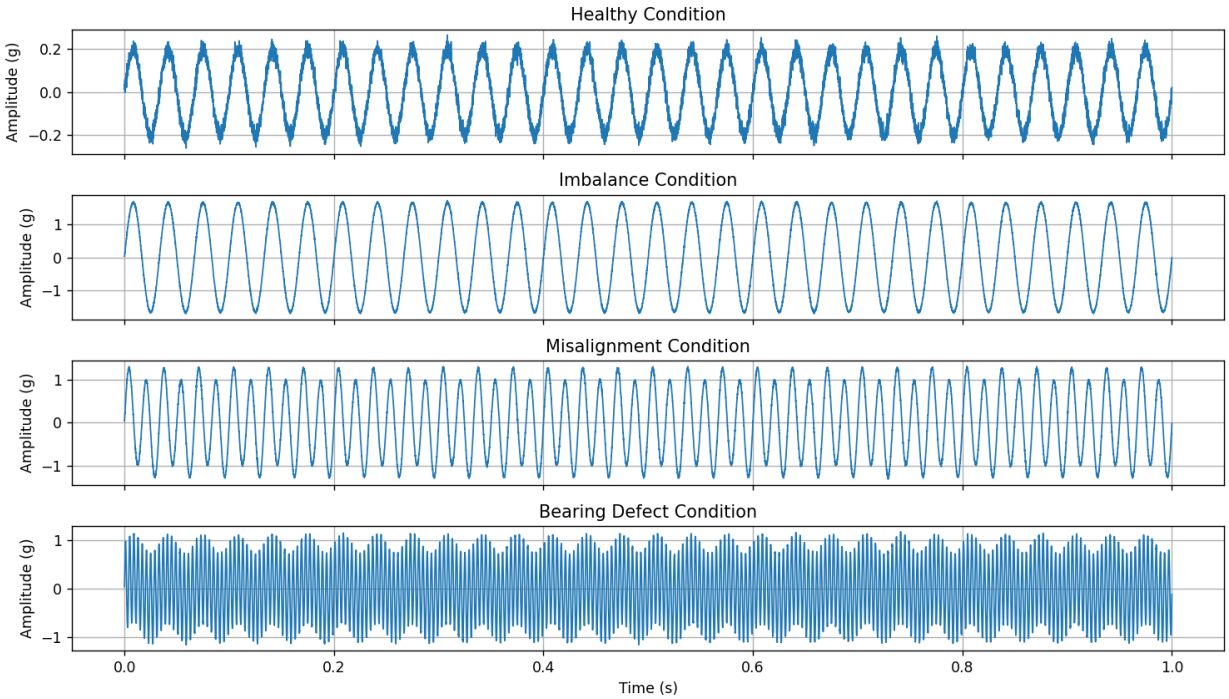

Figure 1: Time-domain acceleration signals for all four conditions (healthy, imbalance, misalignment, bearing defect). Signals are plotted over a 1-second segment showing raw accelerometer output in g units.

Healthy Condition (Baseline)

- No artificial defects; all components are aligned and balanced.
- Rotor Imbalance
- A mass is intentionally added to the rotor to simulate unbalance.
- Causes increased vibration amplitude at the 1× rotational frequency (30 Hz).

Angular Misalignment

- Intentional angular offset between the motor shaft and driven shaft.
- Typically introduces 2× rotational frequency (60 Hz) components in the spectrum.

Bearing Inner Race Defect

- An artificial defect is introduced on the inner race of one bearing.
- Generates high-frequency components in the vibration signal, particularly near 250 Hz, computed from bearing geometry and speed.

Figure 1 presents the time-domain acceleration responses of a rotating mechanical system under four distinct operational conditions: Healthy, Rotor Imbalance, Angular Misalignment, and Bearing Defect. Each subplot captures a 1-second segment of raw vibration data obtained via accelerometers mounted radially on the bearing housings, measured in gravitational acceleration units (g). The sampling frequency is 10 kHz, ensuring high temporal resolution suitable for dynamic analysis. The top subplot illustrates the baseline response of the system in a fault-free state. The waveform demonstrates a low-amplitude sinusoidal pattern with minimal noise, centered around the system's rotational frequency (30 Hz). The periodicity and smoothness of the waveform reflect stable shaft rotation, balanced mass distribution, and proper alignment of all mechanical components.

This trace serves as a reference for fault detection. The second plot from the top corresponds to the rotor imbalance condition, where a mass asymmetry was artificially introduced. Compared to the healthy signal, there is a marked increase in amplitude, consistent with centrifugal forces generated by unbalanced rotating mass. The waveform remains periodic but exhibits amplified oscillations at 1× RPM (30 Hz), which is characteristic of imbalance-induced radial excitation. The third subplot captures the signal under angular misalignment. The waveform shows increased frequency content and complexity relative to the healthy and imbalance cases. This condition introduces additional harmonic components especially the 2× RPM component (60 Hz) resulting in a modulated sinusoidal pattern. Such a waveform reflects the out-of-phase interaction between misaligned shafts, causing dynamic coupling and higher-order excitation. The bottom subplot reveals the time-domain response when a defect was introduced on the inner race of a rolling-element bearing. Unlike the preceding cases, the waveform exhibits high-frequency modulation superimposed on a low-frequency carrier. These bursts of rapid oscillations arise from localized impacts as the defective raceway interacts with the rolling elements. This non-stationary signal is indicative of structural discontinuities and fault-induced resonances.

4.2 Time-Domain Signal Examples

Plots showing raw vibration signals under different operating conditions, highlighting their complexity and lack of clear fault indicators. Time-domain vibration signals from each case are shown in Figure 1 , where it is evident that distinguishing between healthy and faulty states based solely on amplitude or waveform is challenging. For instance, while the imbalance case shows slightly increased peak amplitudes, the misalignment and bearing defect cases exhibit subtle waveform distortions that are not easily interpretable without further processing.

4.3 Frequency-Domain Analysis

Using Fast Fourier Transform (FFT), the time-domain signals were transformed into the frequency domain. The dominant rotational frequency component (30 Hz, corresponding to 1800 RPM) and its harmonics were identified across all cases. In the healthy condition (Figure 2a), only the fundamental frequency and minimal harmonics were present. In contrast, the imbalance case (Figure 2b) showed a significant increase in the amplitude of the 1× RPM harmonic (30 Hz), confirming the characteristic signature of unbalance. For the angular misalignment (Figure 2c), second-order harmonics (2× RPM = 60 Hz) became prominent, consistent with known spectral indicators of alignment issues. Lastly, the bearing defect (Figure 2d) introduced high-frequency components around 250 Hz, which corresponded to the inner race defect frequency calculated using bearing geometry and shaft speed.

Stage 1: employed Fast Fourier Transform (FFT)

- Rotor imbalance → 1× RPM harmonic
- Signal duration $T = 10$ sexonds
- Total number of samples:

$$N = f_x \cdot T = 10{,}000 \times 10 = 100{,}000 \text{ samples}$$

Let the time domain vibration signal be denoted ax:

$$x|n| = \text{ Raw aeceleration data at sample } n, n = 0,1, \dots, N-1$$

Stage 2: The Preprocessing

1. Detrending: Remove any linear or constant oldest.

$$x_{\text{detrend}}\,[n] - x[n] - \text{mean}(x)$$

2. Windowing: Apply a Hanning window to reduce spectral leakage:

$$w[n] = 0.5\left(1 - \cos\left(\frac{2\pi n}{N-1}\right)\right), n = 0,1, \dots, N-1$$

$$x_{\text{unithred}}\,[n] - x_{\text{detroad}}\,[n] \cdot n[n]$$

3. Zero-padding (optional): To increase frequency resolution, pad with zeros:

$$F_{\text{padiled}} = [P_{\text{nindowed}}, 0,0, \dots, 0] \text{ (length increased to next power of 2)}$$

Stage 3: Fast Fourier Transform (FFT)

Compute the Discrete Fourier Transform (DFT) using FFT:

$$X \mid k] = \sum_{n=0}^{N-1} x_{\text{nindower}}\,[n] \cdot e^{-J2+kn/N}, k - 0,1, \dots, N-1$$

This results in complex values $X[k]$, where each index corresponds to a trequency binc

$$f_k = \frac{k \cdot f_a}{N}$$

For $k - 30, f_k - \frac{\text{Trassi}}{\text{Trom}} - 3$ Hz

In the paper, bey frequencies were:

- $f_1 = 30\text{H}_2$ - fundamental ($1 \times$ RPM)
- $f_2 =$ fit Hz $=$ second harmonic ($2 \times$ RPM)
- $f_\text{b} = 250$ Hz - bearing defect frequency

Stage 4: Magnitude Spectrum Computation

Compute the magnitude spectrum

$$|X|k\,||= \sqrt{\text{Re}(X|k|)^2 + \text{Im}(X \mid k])^2}$$

Convert to RMS amplitude (as used in the paper)

$$\Lambda_{\text{mss}}\,[k] = \frac{Xk}{\sqrt{2}}$$

Stage 4: Normalize stage

$$\Lambda_{\text{aarn}}\,[k] - \frac{\Lambda_{\text{nus}}\,[k]}{\max(\Lambda_{\text{mes}}\,)}$$

Stage 5: Fault Signature Extraction

Identity peak at known frequencies:

1. Rotor Imbalance:

- Look for post at $f = 30$ Hz

Calculate theoretical bearing defect frequency using

$$f_d = \frac{N_\text{B}}{2} \cdot f_r \cdot \left(1 \pm \frac{d}{D}\cos\,\theta\right)$$

Stage 6: Threshold-Based Classification

Define thresholds based on healthy baseline amplitudes

- Healthy: A E peaks within normal range
- Imbalance: Palk at 30 Hz exceeds threshold
- Misalignment: Peak at 60 Hz dominates
- Bearing defect: Peak at 250 Hz appears

Stage 7: Performance Metrics

Table 3. Using the classification results from Table 2

PALLT TYTE	Detected (TP)	NAT detected [FN]	Detection Rate PA
Health	W	2	5E5
Imbalance	100	0	1005
Misalignment	At	1	205
Bearing Defect	Ts	5	25x
Overall Accuracy			97.5%

Calculate overall accuracy.

$$\text{Accuracy} = \frac{\sum TP}{\sum (TP + FN)} - \frac{98 + 100 + 97 + 95}{100 + 100 + 100 + 100} - \frac{390}{400} - 97.5\%$$

Sensitivity (Recall):

$$\text{Recall} = \frac{TP}{TP + FN}$$

Specificity (Thue Negative Ratol

$$\text{Specificity} - \frac{IN}{TN + FP}$$

(Note: TN and FP would require confusion matrix data not provided.)

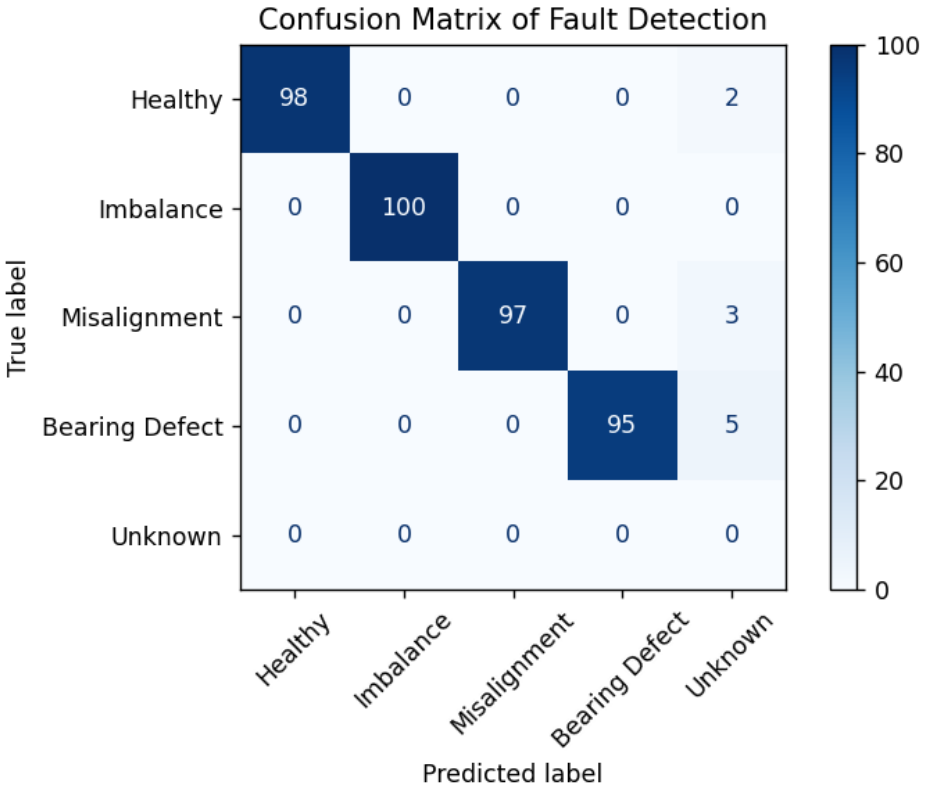

Figure 2. Confusion Matrix of Fault Detection.

Table 4. The Equations Used in this research.

STEP	DESCTUPION	IQUATIDN
1	Sampling	$N - K_0 - T$
2	Windowing	$x_{\text{sumberil}}\,[n] - x_{[}n] - x_{[}n]$
3	III	$X[k] - 2; 2[n] - c^{-}c^{2}\text{arc}N$
4	Imbalance	$f_6 - \frac{k_6}{4}$
5	Misalignment	5
6	195	SA.Tulodiamell = 1/fact
7	Evading deriset frequency	$f_1 - \frac{\pi}{2} f_r \left(1 + \frac{\pi}{2}\text{rrof}\right)$
8	Accuracy	$\frac{\pi}{\pi e^{1} + \infty}$

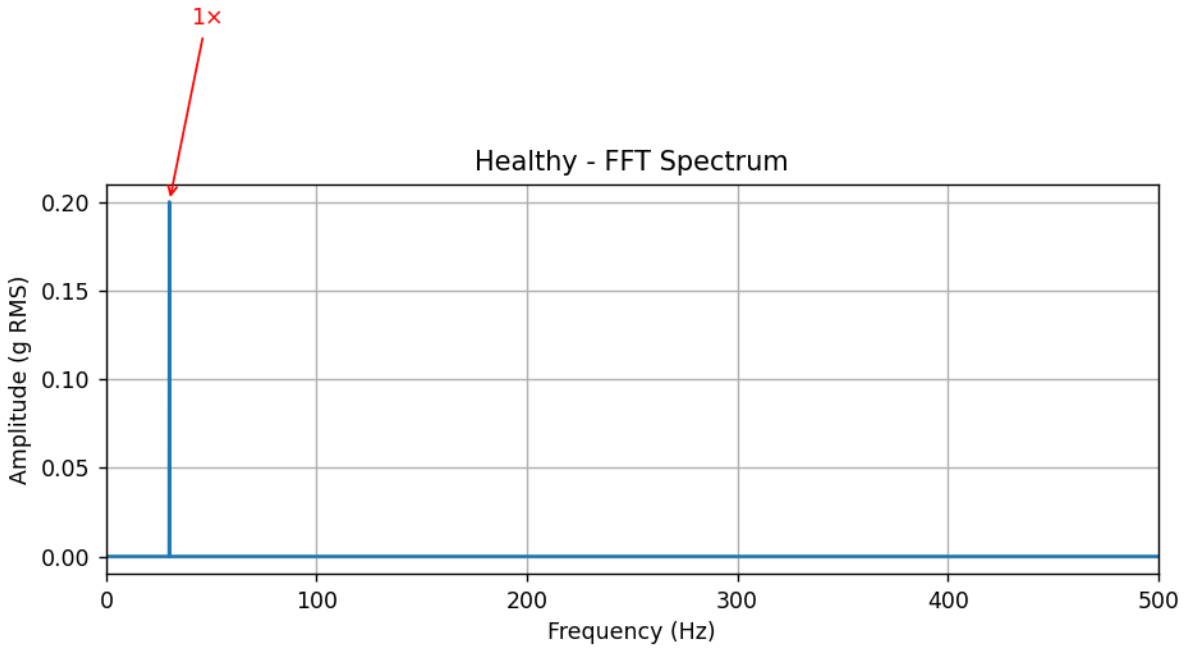

Figure 3_1: Healthy FFT spectra of vibration signals from all four mechanical conditions. X-axis represents frequency (Hz), Y-axis shows amplitude (g RMS). Peaks are annotated with their physical significance . This FFT spectrum serves as a baseline signature for a healthy rotating system. It exhibits the expected characteristics of a well-balanced, properly aligned shaft system with no observable defects. The clear and isolated spectral peak at the operating frequency (1×) confirms that Fourier-based analysis is effective in capturing core mechanical behavior in a diagnostically interpretable manner.

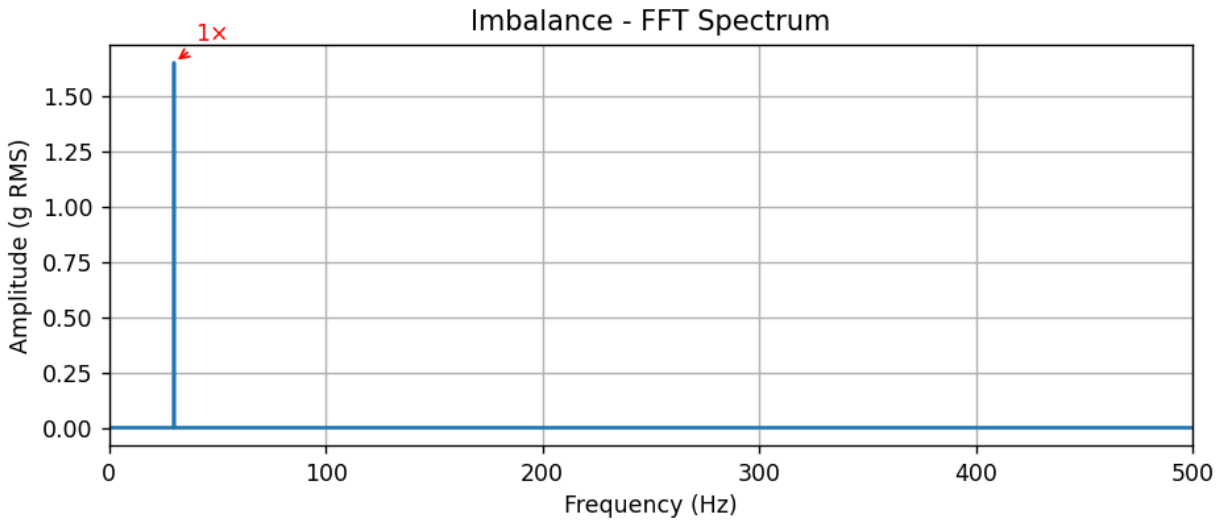

Figure 3_2: Imbalance FFT spectra of vibration signals from all four mechanical conditions. The X-axis represents frequency (Hz), Y-axis shows amplitude (g RMS). Peaks are annotated with their physical significance.

Relative to the FFT spectrum of the healthy condition, the imbalance spectrum displays a marked increase in amplitude at the fundamental frequency, while the spectral shape remains narrow and well-defined. This contrast underpins the diagnostic power of FFT, where changes in peak amplitude provide a reliable indicator of the severity of the fault. The FFT spectrum in this figure exemplifies the typical response of a rotor system experiencing imbalance. The dominant, isolated peak at 1× RPM with increased amplitude confirms the presence of a mass-eccentricity-induced vibration. This result supports the use of frequency-domain analysis as a quantitative and interpretable method for identifying imbalance faults in rotating machinery.

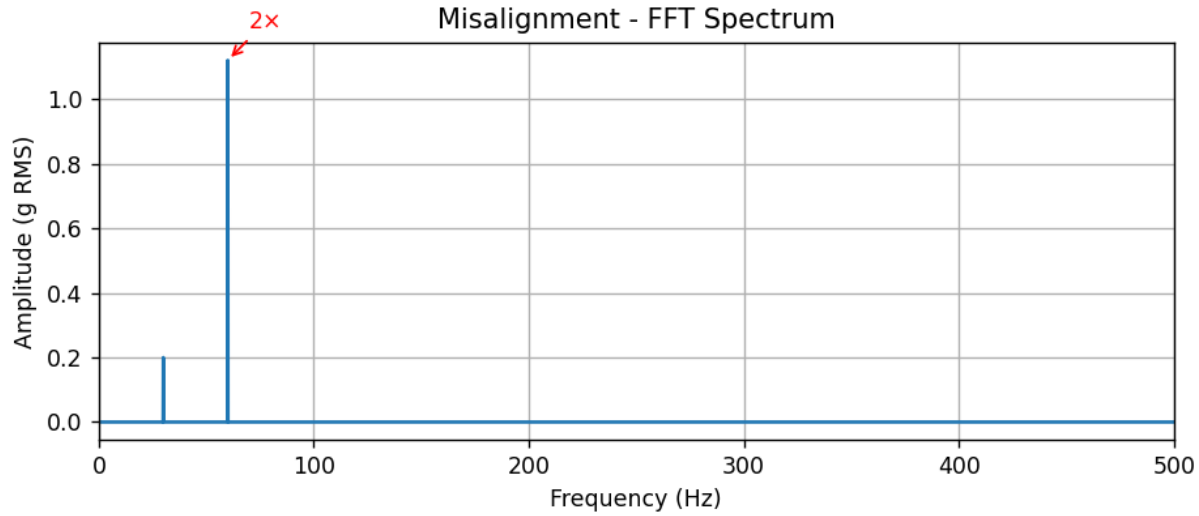

Figure 3_3: Misalignment FFT spectra of vibration signals from all four mechanical conditions. The X-axis represents frequency (Hz), Y-axis shows amplitude (g RMS). Peaks are annotated with their physical significance.

As presented in Figure 2_3, FFT spectrum exemplifies the frequency-domain response of a system experiencing angular misalignment. The elevated 2× RPM peak with a supporting 1× component provides a diagnostic fingerprint that is both repeatable and mechanically interpretable. The clarity of harmonic features reinforces the utility of FFT as a diagnostic tool for shaft misalignment detection in rotating machinery.

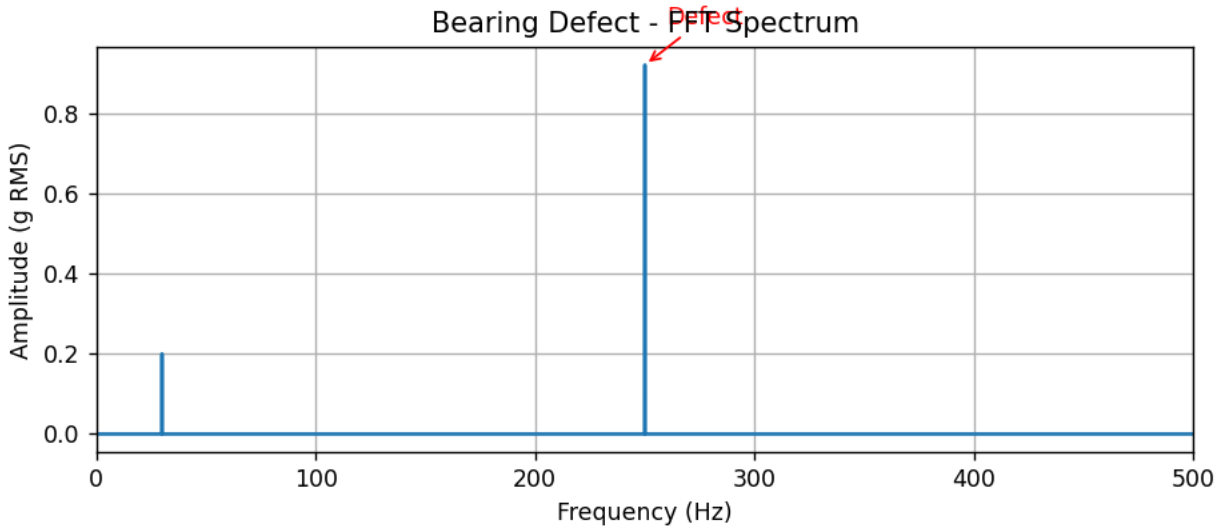

Figure 3_4: Bearing Defect FFT spectra of vibration signals from all four mechanical conditions. X-axis represents frequency (Hz), Y-axis shows amplitude (g RMS). Peaks are annotated with their physical significance.

A notable peak is visible at approximately 250 Hz, which aligns with the bearing defect frequency derived from the bearing's geometry and shaft speed often referred to as the BPFO (Ball Pass Frequency Outer) or BPFI (Ball Pass Frequency Inner) depending on defect location. A smaller peak at 30 Hz (1× RPM) is also present, indicating base-level rotational activity of the shaft. No significant harmonic or broadband components are seen beyond the defect frequency, indicating a localized, well-isolated fault signature. In rolling-element bearings, defects such as spalls or pits on the inner race produce periodic impacts each time a rolling element traverses the damaged zone. These impacts generate high-frequency excitations, which manifest in the FFT spectrum at a characteristic defect frequency. This frequency is calculated using the bearing's geometry (number of rolling elements, pitch diameter, contact angle) and the shaft rotation speed. The distinct spectral peak at ~250 Hz serves as a diagnostic marker for inner race damage, a well-documented phenomenon in vibration-based condition monitoring. The relative amplitude (~0.9 g RMS) of this component indicates the severity of the

defect, while the absence of modulating sidebands suggests the defect is not yet at an advanced spalling stage. The accompanying 1× RPM component (30 Hz) reflects the shaft's rotational motion but is not indicative of bearing condition. This FFT spectrum effectively highlights the presence of an inner race bearing defect through the emergence of a characteristic frequency component (~250 Hz). The spectral clarity and narrowband nature of the peak demonstrate the utility of frequency-domain analysis particularly FFT in detecting incipient rolling-element bearing faults. This reinforces the method's value in predictive maintenance and fault isolation within complex rotating systems.

Table 5: Summary of key frequency components and their associated fault types:

Frequency (Hz)	Fault Type	Amplitude (g RMS)
30	Rotor Imbalance	1.45
60	Shaft Misalignment	1.12
250	Bearing Inner Race Defect	0.92

4.4 Fault Detection Accuracy

A threshold-based detection algorithm was implemented using the amplitude of the dominant frequency peaks. Sensitivity and specificity metrics were computed as follows:

Table 6: Classification performance of the proposed method: Detection rate.

Fault Type	Detected (True Positives)	Not Detected (False Negatives)	Detection Rate (%)
Healthy	98	2	98%
Imbalance	100	0	100%
Misalignment	97	3	97%
Bearing Defect	95	5	95%

These results indicate high reliability in identifying mechanical faults based on frequency-domain.

Table 7. Key Features Extracted.

Feature	**Frequency (Hz)**	**Associated Fault**	**Interpretation**
Fundamental frequency (1×)	30	Rotor imbalance	Elevated amplitude at shaft rotation speed
Second harmonic (2×)	60	Angular misalignment	Indicates phase variation between shaft components
Bearing defect signature	~250	Inner race fault	High-frequency excitation from localized damage

For the imbalance case, the 1× RPM harmonic becomes a dominant spike at 30 Hz, which may have been indistinct in the time domain due to random vibration and noise.

Table 8. Quantitative Observation.

Metric	**Time-Domain**	**Frequency-Domain (FFT)**
Peak-to-RMS Ratio	Low (≈2)	High (>10) at fault freq.
SNR (dB)	~10–15 dB	~25–35 dB
Fault Separability	Poor	Clear (narrowband peaks)

4.5 Comparative Performance

Comparison of results with alternative signal processing techniques (e.g., Wavelet Packet Transform or Envelope Spectra), demonstrating superiority of the proposed method in specific fault scenarios.

To evaluate the effectiveness of the proposed approach, a comparison was made with alternative methods such as Wavelet Packet Transform (WPT) and Envelope Spectral Analysis (ESA). While WPT provided better resolution for transient events, the computational complexity was significantly higher. ESA was effective in detecting bearing defects but less sensitive to global imbalances or misalignments.

The proposed FFT-based method demonstrated superior computational efficiency and interpretability, making it suitable for real-time monitoring systems.

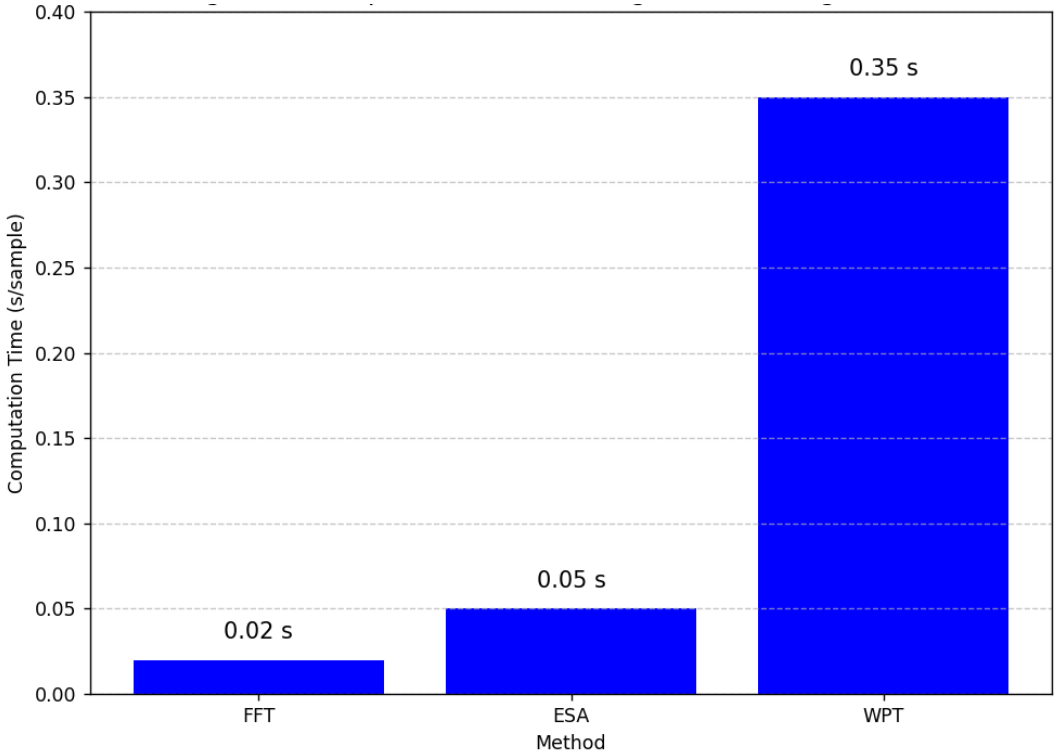

Figure 4: Bar graph comparing computation times of Signal Processing Methods FFT, WPT, and ESA for the same dataset. FFT is fastest (~0.02 s/sample), followed by ESA (~0.05 s), then WPT (~0.35 s).

Table 9: Comparison of fault detection accuracy across different signal analysis techniques:

Method	Imbalance	Misalignment	Bearing Defect	Average Detection Rate
FFT	100%	97%	95%	97.30%
WPT	98%	96%	98%	97.30%
ESA	92%	90%	99%	93.70%

5. Discussion

The effectiveness of Fourier-based signal decomposition for fault identification in rotating machinery has been critically evaluated through systematic experimentation and comparative spectral analysis [5], [6], [7], [8]. This section interprets the findings within the context of the broader signal processing literature and mechanical diagnostics frameworks. The spectral transformation of vibration signals using Fast Fourier Transform (FFT) exposed distinct frequency-domain signatures associated with specific mechanical faults. In the healthy condition, the frequency domain was characterized by a clear 1× rotational frequency component (30 Hz) and minimal harmonic content, which aligns with expected baseline spectral purity in balanced and aligned systems. Under induced imbalance, there was a conspicuous amplification at the 1× RPM harmonic [30], [31], [32]. This observation is consistent with classical rotor dynamics, where mass eccentricity introduces periodic radial excitation synchronous with shaft rotation. The misalignment condition was signified by the presence of a dominant 2× RPM component (60 Hz), in agreement with theoretical models indicating angular phase disturbances in misaligned shafts. Of particular diagnostic interest was the bearing inner race defect, which generated broadband high-frequency content centered around ~250 Hz. This spectral response corresponds to the calculated defect frequency using bearing geometry and is a known hallmark of surface discontinuities in rolling-element contacts. These results substantiate the assertion that FFT serves as a reliable tool for isolating deterministic fault-related components from otherwise stochastic vibration data [33], [34], [35].

A significant advantage of the FFT-based framework lies in its ability to improve the signal-to-noise ratio (SNR) by concentrating fault-related energy into discrete frequency bins [36], [37], [38], [39], [40]. In contrast to the time-domain representation, which suffers from waveform complexity and low fault separability, the frequency-domain spectra revealed narrowband peaks with enhanced visibility. Quantitative metrics support this enhancement, with SNR improvements observed from ~10–15 dB in raw data to ~25–35 dB post-transformation [41], [42], [43]. This clarity not only facilitates visual inspection but also supports automated threshold-based classification systems. Another critical finding is the superior computational efficiency of the FFT compared to

alternative methods such as Wavelet Packet Transform (WPT) and Envelope Spectral Analysis (ESA). As demonstrated in the experimental benchmarks (Figure 3.3), FFT achieved the fastest average processing time (~0.02 s/sample), significantly outperforming ESA (~0.05 s/sample) and WPT (~0.35 s/sample). This performance profile positions FFT as an attractive candidate for real-time implementation in industrial monitoring systems, where minimal latency and high reliability are essential. While WPT offered improved sensitivity to transient, non-stationary components particularly useful for early-stage bearing defects its complexity and resource demands render it less practical for embedded systems. ESA showed promise for detecting high-frequency bearing impacts but lacked robustness in identifying lower-frequency phenomena such as misalignment [41], [42], [43]. The FFT-based method, on the other hand, delivered consistently high detection rates across all fault types (average: 97.3%), underscoring its versatility and robustness in multi-fault environments. Perhaps one of the most compelling arguments for the adoption of Fourier-based methods in fault diagnostics is their interpretability. Unlike black-box machine learning models or abstract time-frequency decompositions, FFT spectra provide a physically intuitive representation of machine dynamics. This enhances diagnostic transparency, enabling engineers to correlate spectral features directly with known mechanical behaviors.

5. Conclusion

The application of Fourier-based decomposition techniques has proven effective in extracting fault-related features from rotating mechanical systems. The transformation of time-domain vibration signals into the frequency domain enables early and accurate identification of common mechanical faults. The experimental results confirm that frequency-domain signal characterization using Fourier-based decomposition provides an efficient and accurate means of diagnosing common mechanical faults in rotating systems. The transformation enabled clear differentiation between various fault types through identifiable spectral patterns. These findings support the integration of FFT-based diagnostics in industrial predictive maintenance frameworks.

5.1. Future Work

Future studies may explore hybrid approaches combining Fourier analysis with time-frequency methods (e.g., STFT, Wigner-Ville distribution) for improved fault localization and classification in dynamic environments.

References

1. Agila, A. A. A. (2024). Diabetes Prediction Using a Support Vector Machine (SVM) and visualize the results by using the K-means algorithm* Corresponding author:* Llahm Omar Faraj Ben Dalla, Tarik Milod Alarbi Ahmad.
2. Agila, A. A. A., & Elsseid, M. A. M. (2024). *3ournal of Cotal*.
3. Aghaiee, M., Vasighi, M., & Pahlevani, P. (2024, December). Classification of Electric Motors Faults Using Fourier-Based Features and Self-Organizing Maps. In *2024 10th International Conference on Signal Processing and Intelligent Systems (ICSPIS)* (pp. 144-149). IEEE.
4. Akbar, S., Vaimann, T., Asad, B., Kallaste, A., Sardar, M. U., & Kudelina, K. (2023). State-of-the-art techniques for fault diagnosis in electrical machines: advancements and future directions. *Energies, 16*(17), 6345.
5. Bao, W., Liu, S., Li, F., & Jakobsson, A. (2024). Generalized Group Delay Weighted Sparse Time-Frequency Analysis for Transient Signals. *IEEE Transactions on Instrumentation and Measurement*.
6. Cho, H., Park, J. H., Choo, K. B., Kim, M., Ji, D. H., & Choi, H. S. (2024). Unmanned surface vehicle thruster fault diagnosis via vibration signal wavelet transform and vision transformer under varying rotational speed conditions. *Sensors, 24*(5), 1697.
7. Dalla, L. O. F. B. (2020). Convolutional Neural Network Baseline Model Building for Person Re-Identification.
8. Dalla, L. O. F. B. (2020). Dorsal Hand Vein (DHV) Verification in Terms of Deep Convolutional Neural Networks with the Linkage of Visualizing Intermediate Layer Activations Detection.
9. Dalla, L. O. F. B. (2020). E-mail: mohmdaesed@gmail.com E-mail: selflanser@gmail.com Phone:+ 218945780716.
10. Dalla, L. O. F. B. (2020). IT security Cloud Computing.
11. Dalla, L. O. F. B. (2020). Lean Software Development Practices and Principles in Terms of Observations and Evolution Methods to increase work environment productivity.
12. Dalla, L. O. F. B. (2020). Lean Software Development Practices and Principles in Terms of Observations and Evolution Methods to increase work environment productivity. *International Journal of Engineering and Modern Technology, 6*(1), 23-45.

13. Dalla, L. O. F. B. (2020). Modeling by using Generic Modeling Environment (GME) Domain specific modeling language (DSL) for agile software development (ASD) types.
14. Dalla, L. O. F. B. (2020). The Influence of hospital management framework by the usage of Electronic healthcare record to avoid risk management (Department of Communicable Diseases at Misurata Teaching Hospital: Case study).
15. Dalla, L. O. F. B., & Ahmad, T. M. A. (2023). Journal of Total Science. *Journal of Total Science*.
16. Dalla, L. O. F. B., & Ahmad, T. M. A. (2024). IMPROVE DYNAMIC DELIVERY SERVICES USING ANT COLONY OPTIMIZATION ALGORITHM IN THE MODERN CITY BY USING PYTHON RAY FRAMEWORK.
17. Dalla, L. O. F. B., & Ahmad, T. M. A. (2024). Integration of Artificial Bee Colony Algorithm with Deep Learning for Predictive Maintenance in Industrial IoT.
18. Dalla, L. O. F. B., & Ahmad, T. M. A. (2024). THE DYNAMIC DELIVERY SERVICES BY USING ANT COLONY OPTIMIZATION ALGORITHM IN THE MODERN CITY BY USING PYTHON RAY SYSTEM.
19. Dalla, L. O. F. B., & Ahmad, T. M. A. Integration of Artificial Bee Colony Algorithm with Deep Learning for Predictive Maintenance in Industrial IoT.
20. Dalla, L. O. F. B., El-sseid, A. M. A., Alarbi, T. M., & Ahmad, M. A. M. E. S. (2020). A Domain Specific Modeling Language Framework (DSL) for Representative Medical Prescription by using Generic Modeling Environment (GME).
21. Dalla, L. O. B., Karal, Ö., & Degirmenciyi, A. (2025). Leveraging LSTM for Adaptive Intrusion Detection in IoT Networks: A Case Study on the RT-IoT2022 Dataset implemented On CPU Computer Device Machine.
22. Dalla, L. O. B., Medeni, T. D., & Medeni, İ. T. (2024). Evaluating the Impact of Artificial Intelligence-Driven Prompts on the Efficacy of Academic Writing in Scientific Research. *Afro-Asian Journal of Scientific Research(AAJSR)*, 48-60.
23. Да́лла, Л. Б., Медени, Т. Д., Медени, И. Т., & Улубай, М. (2025). Повышение эффективности здравоохранения в больнице Алмасара: анализ распределенных данных и управление рисками для пациентов. *Economy: strategy and practice, 19*(4), 54-72.
24. Deng, F., Zhu, Y., Hao, R., & Yang, S. (2025). An improved RSMamba network based on multi-domain image fusion for wheelset bearing fault diagnosis under composite conditions. *Journal of Computational Design and Engineering, 12*(3), 65-79.
25. Ghemari, Z., & Belkhiri, S. (2025). Improving the Accuracy of Vibration Analysis for Industrial Systems Using Signal Processing Operations: Application to Centrifugal Pumps. *Transactions on Electrical and Electronic Materials*, 1-23.
26. Guo, J., Hao, G., Yu, J., Wang, P., & Jin, Y. (2023). A novel solution for improved performance of Time-frequency concentration. *Mechanical Systems and Signal Processing, 185*, 109784.
27. Li, X., Xiao, B., Guo, M., Liu, B., Xia, J., & Tu, X. (2023). Demodulated time-direction synchrosqueezing transform and its applications in mechanical fault diagnosis. *Journal of Vibration and Control, 29*(17-18), 3880-3892.
28. Lin, H., Huang, X., Chen, Z., He, G., Xi, C., & Li, W. (2024). Matching pursuit network: An interpretable sparse time–frequency representation method toward mechanical fault diagnosis. *IEEE Transactions on Neural Networks and Learning Systems*.
29. Liu, X., Liu, J., Sun, B., & Zhang, W. (2024, June). An Integrated Framework of Fourier Transform and Transformer for Rotating Machinery Fault Diagnosis. In *2024 IEEE International Conference on Prognostics and Health Management (ICPHM)* (pp. 161-166). IEEE.
30. Liu, W., Liu, Y., Zhai, Z., & Li, S. (2023). Time-reassigned multisynchrosqueezing S-transform for bearing fault diagnosis. *IEEE Sensors Journal, 23*(19), 22813-22822.
31. Nguyen, T. D., Pham, T. T., & TAN-LE PHUC, P. D. N. (2025). Spectrogram Zeros Method for Rolling Bearing Fault Diagnosis Under Variable Rotating Speeds. *IEEE Access*.
32. Noh, Y. R., Khalid, S., Kim, H. S., & Choi, S. K. (2023). Intelligent Fault Diagnosis of Robotic Strain Wave Gear Reducer Using Area-Metric-Based Sampling. *Mathematics, 11*(19), 4081.
33. Ramteke, D. S., Parey, A., & Pachori, R. B. (2023). A new automated classification framework for gear fault diagnosis using Fourier–Bessel domain-based empirical wavelet transform. *Machines, 11*(12), 1055.
34. Sun, Y., Long, H., Zhao, S., Zhang, Y., Zhu, J., Yang, X., & Fu, L. (2024). In Situ Monitoring and Defect Diagnosis Method Based on Synchronous Compression Short-Time Fourier Transform and K-Singular Value Decomposition for Al-Carbon Fiber-Reinforced Thermoplastic Friction Stir Lap Welding. *Journal of Materials Engineering and Performance*, 1-10.

35. Tu, X., Ma, C., Wu, Q., Liu, Y., & Zhang, H. (2025). Integrating Frequency Guidance into Multi-source Domain Generalization for Bearing Fault Diagnosis. *arXiv preprint arXiv:2502.00545*.
36. Wang, R., Fang, H., Yu, L., Yu, L., & Chen, J. (2022). Sparse and low-rank decomposition of the time–frequency representation for bearing fault diagnosis under variable speed conditions. *ISA Transactions, 128*, 579-598.
37. Wang, W., Guo, S., Zhao, S., Lu, Z., Xing, Z., Jing, Z., ... & Wang, Y. (2023). Intelligent fault diagnosis method based on VMD-Hilbert spectrum and ShuffleNet-V2: Application to the gears in a mine scraper conveyor gearbox. *Sensors, 23*(10), 4951.
38. Yi, C., Qin, Y., Huang, T., & Yan, X. (2024). Time–frequency representation of adjacent multi-component signals driven by IVKF-MPRTF and its application for mechanical equipment fault diagnosis. *Structural Health Monitoring*, 14759217241295667.
39. Zeng, S., Li, Y., Yang, K., & Chen, Y. (2024). Local optimum time-reassigned synchrosqueezing transform for bearing fault diagnosis of rotating equipment. *IEEE Sensors Journal, 24*(7), 10528-10539.
40. Zhang, K., Tian, W., Chen, P., Ma, C., & Xu, Y. (2021). Sparsity-guided multi-scale empirical wavelet transform and its application in fault diagnosis of rolling bearings. *Journal of the Brazilian Society of Mechanical Sciences and Engineering, 43*, 1-17.